

# Teriflunomide preserves peripheral nerve mitochondria from oxidative stress-mediated alterations

Bimala Malla, Samuel Cotten, Rebecca Ulshoefer, Friedemann Paul, Anja E. Hauser, Raluca Niesner, Helena Bros\* and Carmen Infante-Duarte\* 

Ther Adv Chronic Dis

2020, Vol. 11: 1–14

DOI: 10.1177/  
2040622320944773

© The Author(s), 2020.  
Article reuse guidelines:  
sagepub.com/journals-  
permissions

**Abstract:** Mitochondrial dysfunction is a common pathological hallmark in various inflammatory and degenerative diseases of the central nervous system, including multiple sclerosis (MS). We previously showed that oxidative stress alters axonal mitochondria, limiting their transport and inducing conformational changes that lead to axonal damage. Teriflunomide (TFN), an oral immunomodulatory drug approved for the treatment of relapsing forms of MS, reversibly inhibits dihydroorotate dehydrogenase (DHODH). DHODH is crucial for *de novo* pyrimidine biosynthesis and is the only mitochondrial enzyme in this pathway, thus conferring a link between inflammation, mitochondrial activity and axonal integrity. Here, we investigated how DHODH inhibition may affect mitochondrial behavior in the context of oxidative stress. We employed a model of transected murine spinal roots, previously developed in our laboratory. Using confocal live imaging of axonal mitochondria, we showed that in unmanipulated axons, TFN increased significantly the mitochondria length without altering their transport features. In mitochondria challenged with 50  $\mu\text{M}$  hydrogen peroxide ( $\text{H}_2\text{O}_2$ ) to induce oxidative stress, the presence of TFN at 1  $\mu\text{M}$  concentration was able to restore mitochondrial shape, motility, as well as mitochondrial oxidation potential to control levels. No effects were observed at 5  $\mu\text{M}$  TFN, while some shape and motility parameters were restored to control levels at 50  $\mu\text{M}$  TFN. Thus, our data demonstrate an undescribed link between DHODH and mitochondrial dynamics and point to a potential neuroprotective effect of DHODH inhibition in the context of oxidative stress-induced damage of axonal mitochondria.

**Keywords:** dihydroorotate dehydrogenase (DHODH), mitochondria, mitochondrial dynamics, neurodegeneration, oxidative stress, teriflunomide (TFN)

Received: 17 January 2020; revised manuscript accepted: 2 July 2020.

## Introduction

Multiple sclerosis (MS) is a chronic inflammatory disease of central nervous system (CNS) that affects more than 2.5 million people worldwide.<sup>1</sup> In MS, inflammation, demyelination and neurodegeneration are considered to contribute to disease development.<sup>2,3</sup> It is assumed that in MS, a misguided immune response against the CNS is initiated and orchestrated by autoreactive T cells, leading to progressive demyelination, oligodendrocyte injury and axonal loss,<sup>4,5</sup> that affect not only the white but also the grey matter.<sup>6</sup>

The mechanisms by which neuroinflammation and myelin damage lead to neurodegeneration have not been fully elucidated; however, the sustained release of reactive oxygen species (ROS) and nitrogen species (NOS) by macrophages and activated microglia during inflammation appears to contribute to the damaging cascade.<sup>7–9</sup> Also in cortical lesions, demyelination appears to be associated with excessive oxidative damage.<sup>10</sup> Mitochondrial pathology and subsequent focal axonal injury appears also to be triggered by inflammation-associated ROS and NOS and to

Correspondence to:  
**Carmen Infante-Duarte**  
Institute for Medical Immunology, Charité – Universitätsmedizin Berlin and Experimental & Clinical Research Center (ECRC), MDC for Molecular Medicine and Charité – Universitätsmedizin, Campus Virchow Klinikum, Augustenburger Platz 1, Berlin 13353, Germany  
[carmen.infante@charite.de](mailto:carmen.infante@charite.de)  
**Bimala Malla**  
**Samuel Cotten**  
**Rebecca Ulshoefer**

**Helena Bros**

Charité –  
Universitätsmedizin  
Berlin, corporate member  
of Freie Universität Berlin,  
Humboldt-Universität zu  
Berlin and Berlin Institute  
of Health, Institute for  
Medical Immunology,  
Berlin, Germany

**Friedemann Paul**

NeuroCure Clinical  
Research Center, Charité  
– Universitätsmedizin  
Berlin and Experimental  
& Clinical Research  
Center (ECRC), Max  
Delbrueck Center  
(MDC) for Molecular  
Medicine, Berlin,  
Germany and Charité  
– Universitätsmedizin  
Berlin, Berlin, Germany

**Anja E. Hauser**

Medizinische Klinik  
mit Schwerpunkt  
Rheumatologie  
und Klinische  
Immunologie, Charité  
– Universitätsmedizin  
Berlin, corporate member  
of Freie Universität Berlin,  
Humboldt – Universität zu  
Berlin, and Berlin Institute  
of Health, Berlin, Germany  
Deutsches Rheuma-  
Forschungszentrum,  
Berlin, Germany

**Raluca Niesner**

Dynamic and Functional  
in vivo Imaging,  
Deutsches Rheuma-  
Forschungszentrum,  
Berlin, Germany and  
Veterinary Medicine,  
Freie Universität Berlin,  
Germany

\*These senior authors  
contributed equally to the  
work

be independent of demyelinating processes.<sup>11</sup> Axonal mitochondrial damage is an early sign of neurodegeneration that precedes and contributes to focal and reversible alterations in axon morphology. The alterations of the mitochondrial function within axons have been proposed to occur in the early stages of the disease, even before demyelination,<sup>11,12</sup> and to precede neuronal death.<sup>13–16</sup> In autopsied tissue from chronic progressive MS, respiratory deficient neurons were detected both in white and grey matter. Respiration deficits were shown to be caused by multiple deletions of mitochondrial DNA, probably subsequent to inflammation and oxidative stress, that contributed to an enhanced susceptibility of axons and neurons to additional damaging insults.<sup>17</sup> In this line, we and others have shown that oxidative stress disrupts the transport of mitochondria in the axon.<sup>14,18</sup> Hence, mitochondrial dysfunction is considered as one of the major contributors of neuroaxonal damage in MS.

With regard to MS management and treatment, teriflunomide (TFN) (Aubagio; Genzyme, Cambridge, MA, USA) is a once-daily oral immunomodulatory drug for the treatment of patients with relapsing forms of MS.<sup>19</sup> TFN has been shown to reduce relapse events and increase the periods of remission.<sup>20,21</sup>

TFN seems to exert its therapeutic effect by non-competitively and reversibly inhibiting the mitochondrial respiratory chain-associated enzyme dihydroorotate dehydrogenase (DHODH).<sup>22–25</sup> DHODH is involved in *de novo* pyrimidine biosynthesis, thus limiting lymphocytic proliferation and inflammation. However, whether the inhibition of DHODH alone may affect neuronal mitochondria remains uncertain. Importantly, a very recent retrospective, single-center, observational study indicated that the effect of TFN in reducing cortical grey matter atrophy is superior to the effect of the anti-oxidative and anti-inflammatory dimethyl fumarate.<sup>26</sup> Moreover, it has been reported that TFN penetrates into the CNS and exerts its effect directly within the brain.<sup>27</sup> Thus, TFN may indeed have the potential to affect axonal mitochondria directly.

To explore the possible effects of TFN on the nervous system, we have used in this study a previously established model of explanted spinal roots, in which we had shown that mitochondria

undergo a series of alterations in response to oxidative stress.<sup>18,28</sup>

In patients treated daily with 14 mg TFN, average steady-state maximum TFN concentration ( $C_{max}$ ) in plasma is 168  $\mu\text{M}$ .<sup>29</sup> The half maximum concentration ( $IC_{50}$ ) for interaction of TFN with human DHODH is 1  $\mu\text{M}$ <sup>30,31</sup> and 50–100  $\mu\text{M}$  is considered sufficient to inhibit protein tyrosine kinase *in vitro*.<sup>29,31</sup> Moreover, a study assessing the effect of TFN on eryptosis indicated that concentrations ranging from 3.7 to 37  $\mu\text{M}$  TFN might compensate oxidative stress-mediated erythrocyte changes *in vitro*.<sup>32</sup> In rats, it has been shown that after one single injection of 10  $\mu\text{g/g}$  TFN, approximately 2–4% of the blood concentration was found in the brain (~2.5–4.1  $\mu\text{M}$ ).<sup>30</sup> Although an extrapolation to the human reality is not exact, we could suppose in treated patients a TFN concentration within the nervous system of about 3–7  $\mu\text{M}$ . Therefore, in our study, we investigated the effect of TFN on oxidative stress-induced mitochondrial alterations in murine root explants using three different TFN concentrations, 1  $\mu\text{M}$ , 5  $\mu\text{M}$  and 50  $\mu\text{M}$ .

We show that TFN is able to prevent mitochondrial alterations induced by hydrogen peroxide ( $\text{H}_2\text{O}_2$ ), suggesting that TFN has additional therapeutically relevant properties related to mitochondrial protection in axons.<sup>31</sup>

## Materials and methods

### Ethics

All experimental procedures were approved by the local authority on animal studies in Berlin (Landesamt für Gesundheit und Soziales Berlin; ID: T0002/10). Animal studies were performed in strict accordance with the European Communities Council Directive of 22 September 2010 (2010/63/EU).

### Solutions and drugs

Explanted roots were bathed in artificial cerebrospinal fluid (aCSF) containing the following: solution I: 124 mM sodium chloride (NaCl), 1.25 mM sodium dihydrogen phosphate ( $\text{NaH}_2\text{PO}_4$ ), 10.0 mM glucose, 1.80 mM magnesium sulphate ( $\text{MgSO}_4$ ), 1.60 mM calcium chloride ( $\text{CaCl}_2$ ), 3.00 mM potassium chloride (KCl);

solution II: 26.0mM sodium bicarbonate ( $\text{NaHCO}_3$ ). Solutions I and II were mixed immediately before use. Hydrogen peroxide ( $\text{H}_2\text{O}_2$ ; 30% w/w in  $\text{H}_2\text{O}$ , with a stabilizer) and dimethyl sulfoxide (DMSO) were purchased from Sigma-Aldrich. To induce oxidative stress, explanted roots were incubated with  $50\mu\text{M}$  of  $\text{H}_2\text{O}_2$  dissolved in aCSF for 30 min. TFN was applied at different concentrations along with  $\text{H}_2\text{O}_2$  for 30 min. TFN was provided in powder form by the manufacturer (Sanofi Genzyme), which was dissolved in DMSO and stored at  $-20^\circ\text{C}$ .

#### *Preparation of ventral spinal roots*

Ventral spinal roots were prepared as described in our previous work.<sup>18,28,33</sup> Briefly, C57BL/6 mice at least 3 weeks of age were anesthetized with isoflurane prior to cervical dislocation. After separating the connective tissue and exposing the dorsal side of the spinal cord, an initial sectioning was made at the thoracic level, which proceeded in a rostral to caudal direction until the last vertebrae. The spinal cord was lifted gently to expose the ventral roots, which were cut distal to the spinal cord but before the formation of the peripheral nerves. The explanted spinal cord with attached roots was transferred to aCSF saturated with carbogen (95% oxygen [ $\text{O}_2$ ]; 5% carbon dioxide [ $\text{CO}_2$ ]). Under a dissecting microscope, lumbar ventral roots of at least 0.8cm were selected and separated from the spinal cord.

#### *Labeling of mitochondria*

All experimental incubations were conducted in a submerged incubation chamber (Brain Slice Keeper- BSK6-6; Scientific Systems Design Inc., Ontario, Canada), which allows for multiple treatment conditions and continuous carbogen perfusion of each submersion well. Transected ventral spinal roots were transferred to fresh aCSF containing 300nM, MitoTracker CMTMRos orange (Life Technologies, Darmstadt, Germany) for 30 min and washed with aCSF.

#### *Confocal microscopy*

Explanted ventral roots were placed onto a glass coverslip and transferred to an imaging chamber filled with carbogenated aCSF. To prevent movement of the roots during imaging, a custom-built net was placed on the top of the roots.<sup>28</sup> For all imaging experiments, we used an inverted

laser-scanning confocal microscope adapted for live cell imaging (LSM 710; Carl Zeiss, Jena, Germany). MitoTracker Orange was excited with a diode-pumped solid state (DPSS) laser at 561nm. After finding the middle of the root,  $3 \times 60$ -sec videos (2sec/frame) with a resolution of  $512 \times 512$  pixels were acquired in three separate regions of interest (ROI) according to the following criteria: (a) there was a clearly defined node of Ranvier; (b) there were visibly labeled mitochondria; and (c) the areas were no closer than 0.2 cm from the ends of the roots. Typically, the first ROI was located at the middle of the root, whereas the following two were to the right and left of the middle region.

#### *Analysis of mitochondrial dynamics*

Mitochondrial morphology was assessed using an automated analysis function of the Volocity 6.3 software (Perkin Elmer, Rodgau, Germany). The first frame of every video was used for analysis. Shape factor, a measure of circularity ranging from 0 and 1 (closer to '0' was a longer mitochondrion, whereas '1' was a perfect circle), length ( $\mu\text{m}$ ) and area of individual mitochondria were quantified for assessing change in mitochondrial morphology.

Mitochondrial transport was quantified in terms of the number of moving mitochondria, velocity, displacement, and track length of moving mitochondria. Displacement is the measure of shortest distance in  $\mu\text{m}$ , covered by a mitochondrion; it was measured as a straight line from the start to the end position during the 30 frames. Track length is the measure of real distance path longitude followed by the mitochondrion. Mitochondria were tracked manually using Volocity 6.3 software (Perkin Elmer, Rodgau, Germany). Any mitochondrion with a displacement of at least  $1\mu\text{m}$  was considered 'mobile'. Measurements from three ROI were averaged for each root.

In total, 15 different mice in 15 independent experiments were investigated. Depending on the quality of the explants, at least five independent roots and 15 ROI per culturing condition were included into the analysis (usually up to three different ROI per root). Specifically, 39 and 44 ROI were analyzed for the untreated group and  $\text{H}_2\text{O}_2$  treated groups, respectively; 15–21 ROI were used to investigate treatments with  $\text{H}_2\text{O}_2 + \text{TFN}$ .

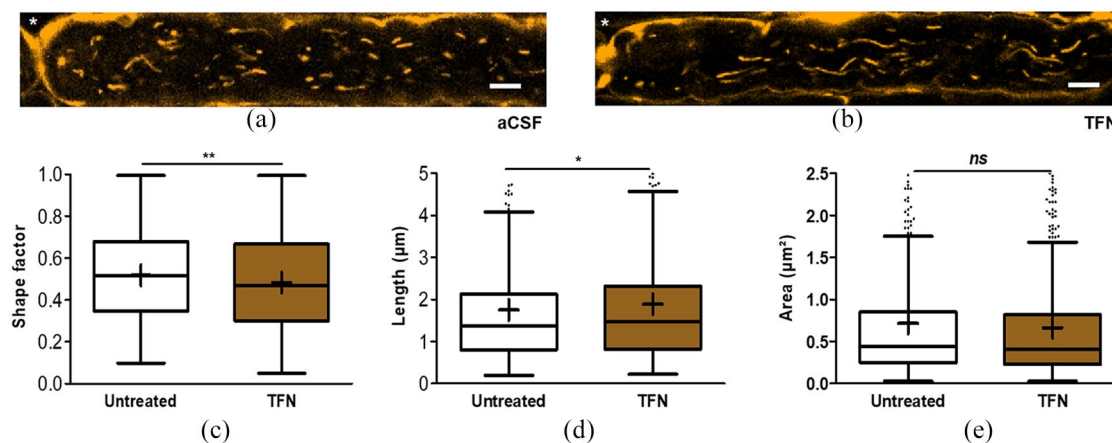


**Figure 1.** Teriflunomide (TFN) affected mitochondrial shape and length in untreated root explants.

(a) Representative confocal picture of the mitochondria within single axons in an untreated peripheral root explant and (b) treated with TFN. The node of Ranvier is located on the left side shown with an asterisk (\*). Scale bar: 5  $\mu\text{m}$ . (c) Shape factor (circularity), (d) length and (e) area of mitochondria. The mitochondrial shape and length is significantly less round and longer after treating the axons with TFN (50  $\mu\text{M}$ ).

Graphs are shown in Tukey boxplots, where the central line denotes the median; the lower and upper boundaries denote the first and third quartile, and the whiskers denote the spread of the data.

Inside the box, '+' delineates the mean.

*ns*, not significant statistically.

\* $p < 0.05$ , \*\* $p < 0.01$ .

For the morphological investigations, the number of mitochondria in the selected ROI were 2586, 2860, 1306, 875 and 1550 for untreated,  $\text{H}_2\text{O}_2$ -treated,  $\text{H}_2\text{O}_2 + \text{TFN}$  (1  $\mu\text{M}$ ),  $\text{H}_2\text{O}_2 + \text{TFN}$  (5  $\mu\text{M}$ ) and  $\text{H}_2\text{O}_2 + \text{TFN}$  (50  $\mu\text{M}$ ), respectively. Analyses of motility included 201, 70, 83, 52 and 64 motile mitochondria for each of the above-mentioned groups.

For the comparison of untreated *versus* TFN-treated nerves, four independent experiments were performed. Analyses include 12 ROI per condition. In total, 568 and 672 individual mitochondria were analyzed, respectively.

#### Quantification of relative change in intracellular ROS

The fluorescence intensity of the MitoTracker Orange was quantified as a measure of intracellular ROS as described by Kweon *et al.*,<sup>34</sup> The images obtained from confocal microscopy were used for the quantification of mitochondrial fluorescence intensity using Image J software.

#### Statistical analysis and data representation

The data were analyzed with Prism 5.01 software (GraphPad, CA, USA). All datasets were subjected first to D'Agostino and Pearson omnibus

K2 normality test for Gaussian distribution. All data fitting the criteria for a normal distribution were subsequently analyzed using a one-way analysis of variance (ANOVA) with Bonferroni's *post hoc* test. All data following a non-parametric distribution were analyzed using a Kruskal–Wallis test followed by a *post hoc* Dunn's multiple comparisons test. All data are given in mean  $\pm$  SD.

Data are shown in Tukey box and whisker plots. The box and whisker plot shows simultaneously the minimum, first quartile, mean (+), median (dissecting line inside the box), third quartile, and maximum of the data set. Whiskers indicate variability outside the upper and lower quartiles. Outliers are plotted as individual dots that are in line with whiskers. The mean + SD values are given in the corresponding tables.

## Results

#### TFN altered mitochondrial dynamics in peripheral root explants

We labelled peripheral root mitochondria with MitoTracker Orange and the explants were imaged for morphological investigation (Figure 1a, b). Then, the effects of TFN on mitochondrial morphology and transport in unmanipulated explanted roots were investigated. Explanted roots were

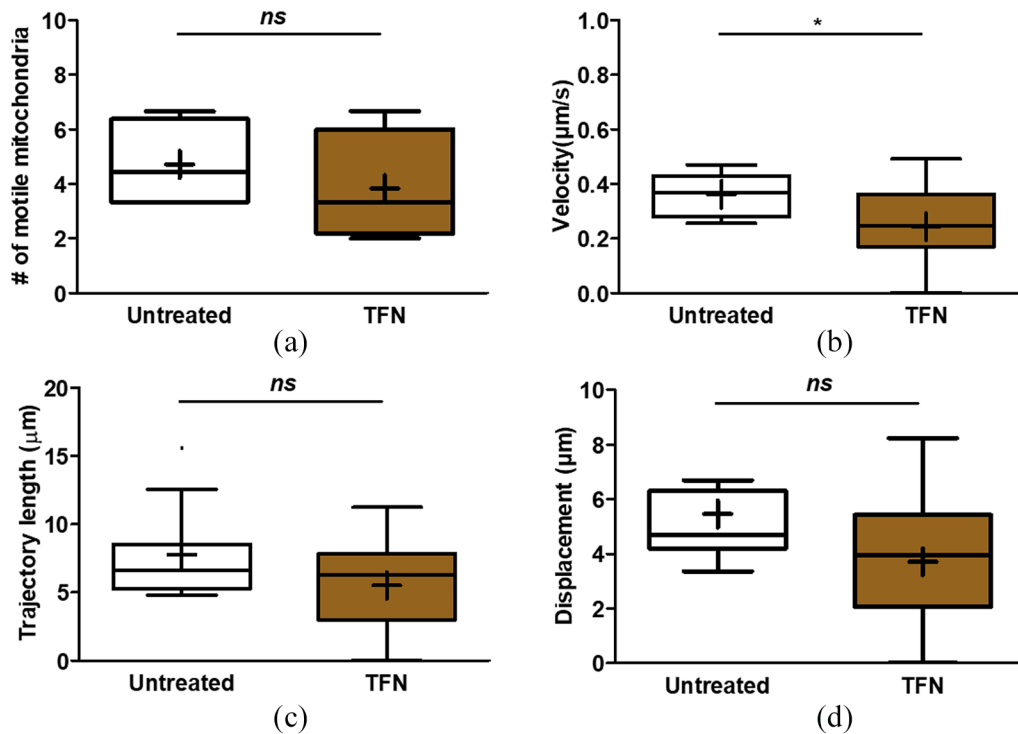


**Figure 2.** Teriflunomide (TFN) reduced mitochondrial velocity without influencing motile number, trajectory length and displacement of mitochondria in untreated root explants.

(a) Number of moving mitochondria per root during 1 min in untreated *versus* TFN-treated roots, (b) velocity of mitochondrial transport, (c) length of the mitochondrial trajectories and (d) displacement (final position minus initial position) of mitochondria.

Graphs are shown in Tukey boxplots, where the central line denotes the median; the lower and upper boundaries denote the first and third quartile, and the whiskers denote the spread of the data. Inside the box, '+' delineates the mean.

*ns*, not significant statistically.

\* $p < 0.05$ .

incubated in the presence or absence of  $50\mu\text{M}$  TFN. TFN treatment resulted in a statistically significant decrease in mitochondrial circularity (Figure 1c) and an increase in mitochondrial length (Figure 1d). There were no significant changes in mitochondrial area (Figure 1e) after TFN treatment compared with the untreated controls.

For mitochondrial motility, TFN did not significantly change the number of motile mitochondria (Figure 2a) as well as the distance covered by the mitochondria (Figure 2c, d). However, it induced a significant reduction of the mean velocity of mitochondrial transport (Figure 2b). Corresponding statistical information is summarized in Table 1.

#### *TFN prevented oxidative stress-induced morphological changes in mitochondria*

We previously reported that oxidative stress leads to substantial changes to both morphology and

transport of axonal mitochondria.<sup>18</sup> Here, we investigated whether TFN, applied together with  $\text{H}_2\text{O}_2$ , would be able to prevent these effects. We treated the roots with  $50\mu\text{M}$   $\text{H}_2\text{O}_2$  (both groups containing the vehicle DMSO), and 3 different concentrations of TFN: 1, 5 and  $50\mu\text{M}$  in aCSF (Figure 3a–e). We analyzed a total of 39 untreated ROI, 44 ROI treated with  $\text{H}_2\text{O}_2$ , and 18, 15 and 21 ROI treated with  $1\mu\text{M}$ ,  $5\mu\text{M}$  and  $50\mu\text{M}$  TFN in the presence of  $50\mu\text{M}$   $\text{H}_2\text{O}_2$ , respectively, from 15 independent experiments. Consistent with our previous findings, we observed that treatment with  $50\mu\text{M}$   $\text{H}_2\text{O}_2$  induced an overall increase of mitochondrial circularity and a corresponding decrease in mitochondrial length and area. In particular, mitochondria were significantly more circular (Figure 3f), shorter (Figure 3g) and smaller (Figure 3h) than their untreated counterparts.

In the presence of  $1\mu\text{M}$  TFN, the shape factor of the mitochondria was reduced, that is,

**Table 1.** Summary of morphology and motility parameters of mitochondria in untreated and teriflunomide-treated peripheral root explants.

	<i>n</i> =	Shape factor	Length (μm)	Area (μm <sup>2</sup> )	No. of motile mitochondria	Velocity (μm/s)	Trajectory length (μm)	Displacement (μm)
Untreated	39	0.52 ± 0.21	1.75 ± 1.52	0.77 ± 0.86	4.72 ± 1.67	0.36 ± 0.07	7.77 ± 3.26	5.46 ± 2.39
TFN (50 μM)	12	0.48 ± 0.23	1.89 ± 1.67	0.66 ± 0.82	3.83 ± 2.06	0.24 ± 0.15	5.51 ± 3.49	3.71 ± 2.43
Mann-Whitney test		**	*	>0.1	>0.1	*	>0.1	>0.1

Values are shown as mean ± SD.  
\**p* < 0.05; \*\**p* < 0.01

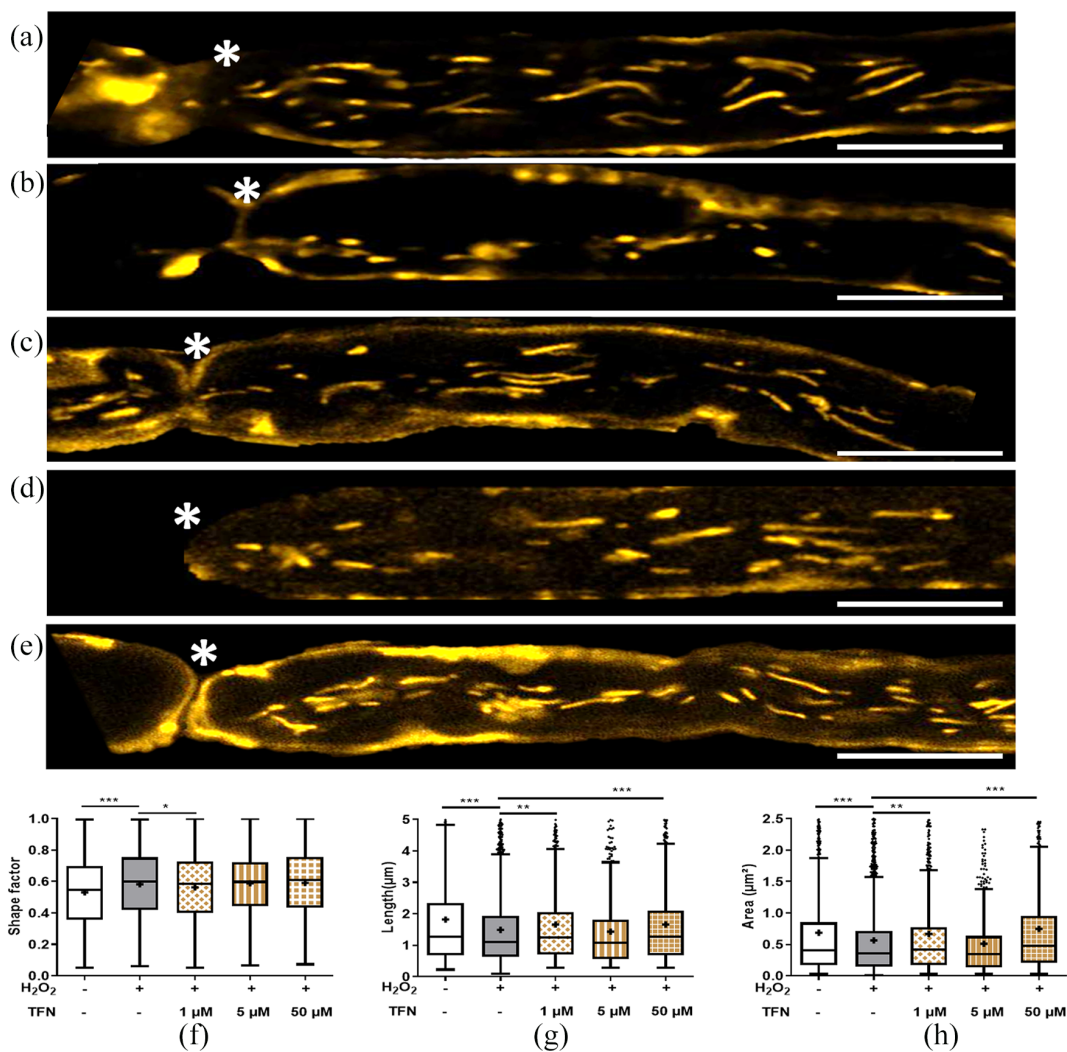


**Figure 3.** Mitochondrial morphology altered during oxidative stress with/out teriflunomide (TFN) treatment. Representative image of mitochondria in (a) untreated, (b) hydrogen peroxide (H<sub>2</sub>O<sub>2</sub>)-treated, and (c, d, and e) H<sub>2</sub>O<sub>2</sub>-TFN-treated, where TFN was 1, 5 and 50 μM, respectively, in murine peripheral root explants. Scale bar: 10 μm. (f) Change in mitochondrial shape factor, (g) length, and (h) area of mitochondria in the presence of H<sub>2</sub>O<sub>2</sub> with or without TFN. Graphs are shown in Tukey boxplots, where the central line denotes the median; the lower and upper boundaries denote the 1st and 3rd quartile, and the whiskers denote the spread of the data. Inside the box, '+' delineates the mean. \**p* < 0.05, \*\**p* < 0.01, \*\*\**p* < 0.001.

**Table 2.** Summary of shape factor, length and area of mitochondria under H<sub>2</sub>O<sub>2</sub> treatment alone, and with 50 μM H<sub>2</sub>O<sub>2</sub> in the presence of 1 μM, 5 μM and 50 μM teriflunomide.

	<i>n</i> =	Shape factor	KW test	Length (μm)	KW test	Area (μm <sup>2</sup> )	KW test
Untreated	39	0.53 ± 0.22	↑ ***	1.82 ± 1.79	↑ ***	0.69 ± 0.92	↑ ***
H <sub>2</sub> O <sub>2</sub> -treated	44	0.58 ± 0.21	↓ ↓ ↓ ↓	1.49 ± 1.29	↓ ↓ ↓ ↓	0.57 ± 0.65	↓ ↓ ↓ ↓
H <sub>2</sub> O <sub>2</sub> + TFN (1 μM)	18	0.57 ± 0.21	↓ ↓ ↓ ↓ *	1.66 ± 1.50	↓ ↓ ↓ ↓ **	0.67 ± 0.85	↓ ↓ ↓ ↓ **
H <sub>2</sub> O <sub>2</sub> + TFN (5 μM)	15	0.59 ± 0.19	↓ ↓ ↓ ↓ >0.1	1.43 ± 1.29	↓ ↓ ↓ ↓ >0.1	0.51 ± 0.69	↓ ↓ ↓ ↓ >0.1
H <sub>2</sub> O <sub>2</sub> + TFN (50 μM)	21	0.59 ± 0.21	↓ ↓ ↓ ↓ >0.1	1.66 ± 1.42	↓ ↓ ↓ ↓ ***	0.75 ± 0.93	↓ ↓ ↓ ↓ ***

KW, Kruskal–Wallis; H<sub>2</sub>O<sub>2</sub>, hydrogen peroxide.  
 Values are shown as mean ± SD.  
 \**p* < 0.05; \*\**p* < 0.01; \*\*\**p* < 0.001.

mitochondria became elongated or rod-shaped (Figure 3f). In contrast, no effects were observed at higher concentration of TFN. Moreover, the lowest and highest TFN concentrations (1 μM and 50 μM) induced a significant increase in mitochondrial length (Figure 3g) and area (Figure 3h), in comparison with the mitochondria exposed to H<sub>2</sub>O<sub>2</sub> alone. Paradoxically, treatment with 5 μM TFN with 50 μM H<sub>2</sub>O<sub>2</sub>, showed no statistically significant effect on H<sub>2</sub>O<sub>2</sub>-induced morphological alterations (Figure 3f–h) (0.59 ± 0.19 shape factor, 1.43 ± 1.29 μm length, and 0.51 ± 0.69 μm<sup>2</sup> area; Kruskal-Wallis test followed by Dunn's *post hoc* test *p* > 0.1 in all cases).

Corresponding statistical information is summarized in Table 2.

#### *TFN prevented oxidative stress-induced changes in mitochondrial motility*

To investigate TFN effects on mitochondrial motility, roots were treated either with aCSF, 50 μM H<sub>2</sub>O<sub>2</sub> (both groups containing DMSO) or 50 μM H<sub>2</sub>O<sub>2</sub> in the presence of three different concentrations of TFN: 1, 5 and 50 μM (Figure 4a–e). We observed that H<sub>2</sub>O<sub>2</sub> treatment led to an overall decrease in the number of motile mitochondria (Figure 4f). In addition, the moving mitochondria had lower mean velocity (Figure 4g), trajectory length (Figure 4h), and displacement (Figure 4i) than the untreated mitochondria.

Again, the lowest and highest TFN concentration (1 μM and 50 μM) restored the motility-related parameters to control levels, except for the mitochondrial velocity with 50 μM TFN, when compared with the mitochondria exposed to H<sub>2</sub>O<sub>2</sub> alone; for the number of moving mitochondria (Figure 4f), velocity (Figure 4g), trajectory (Figure 4h), and displacement (Figure 4i). In contrast, 5 μM TFN had no effect. Corresponding statistical information is summarized in Table 3.

#### *TFN prevented change in mitochondrial oxidation potential in peripheral nerve explants during oxidative stress*

MitoTracker Orange CMTMRos is a reduced, non-fluorescent dye that fluoresces on oxidation. Thus, in conditions of high oxidative stress, mitochondria acquire higher fluorescence intensity.<sup>34</sup> We observed that fluorescence intensity was higher in H<sub>2</sub>O<sub>2</sub>-treated roots compared with untreated controls (Figure 5). In the presence of 1 μM TFN, the fluorescence intensity in the mitochondria was reduced, approaching the values of the untreated axons (Table 4), suggesting that the H<sub>2</sub>O<sub>2</sub>-mediated increase in the oxidation potential could be prevented by TFN. In contrast, no effect was observed at 5 or 50 μM TFN. Corresponding statistical information is summarized in Table 4.

## Discussion

While current treatments for MS focus on reducing inflammation *via* modulation of the

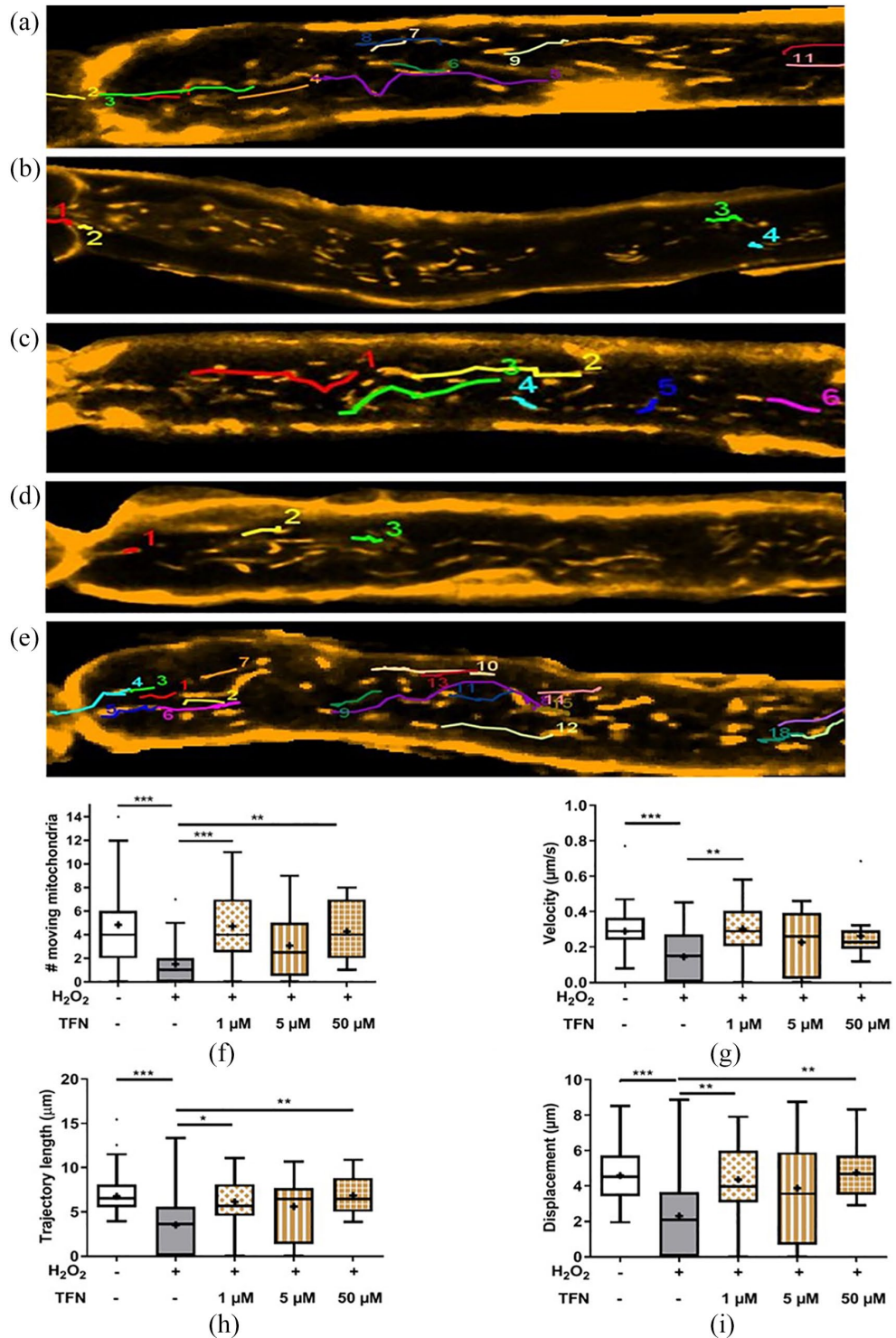


**Figure 4.** Mitochondrial motility altered during oxidative stress with or without teriflunomide (TFN) treatment. A representative image of mitochondrial tracking in (a) untreated, (b) hydrogen peroxide (H<sub>2</sub>O<sub>2</sub>)-treated, and (c, d, and e) H<sub>2</sub>O<sub>2</sub>-TFN treated where TFN was 1, 5 and 50 μM, respectively, in murine peripheral root explants. (f) Number, (g) velocity, (h) trajectory, and (i) displacement of mitochondria.

Graphs are shown in Tukey boxplots, where the central line denotes the median; the lower and upper boundaries denote the first and third quartile and the whiskers denote the spread of the data. Inside the box, '+' delineates the mean.

\**p* < 0.05; \*\**p* < 0.01; \*\*\**p* < 0.001.



**Table 3.** Summary of mitochondrial motility, velocity, displacement and trajectory length under H<sub>2</sub>O<sub>2</sub> treatment alone, and along with different concentrations of teriflunomide.

	<i>n</i> =	# motile mitochondria (axon)	KW test	Velocity (µm/s)	KW test	Trajectory length (µm)	KW test	Displacement (µm)	KW test
Untreated	39	4.85 ± 3.72 (39)	***	0.29 ± 0.14	***	6.77 ± 3.13	***	4.59 ± 2.16	***
H <sub>2</sub> O <sub>2</sub> -treated	44	1.52 ± 1.71 (39)		0.15 ± 0.14		3.53 ± 3.67		2.30 ± 2.60	
H <sub>2</sub> O <sub>2</sub> + TFN (1 µM)	18	4.71 ± 3.08 (21)	***	0.30 ± 0.13	**	6.13 ± 2.59	*	4.37 ± 1.97	**
H <sub>2</sub> O <sub>2</sub> + TFN (5 µM)	15	3.08 ± 2.75 (12)	>0.1	0.23 ± 0.17	>0.1	5.61 ± 3.69	>0.1	3.87 ± 2.96	>0.1
H <sub>2</sub> O <sub>2</sub> + TFN (50 µM)	21	4.27 ± 2.34 (15)	**	0.26 ± 0.13	>0.1	6.84 ± 2.15	**	4.75 ± 1.45	**

KW, Kruskal-Wallis; H<sub>2</sub>O<sub>2</sub>, hydrogen peroxide. Values are shown as mean ± SD. \**p* < 0.05; \*\**p* < 0.01; \*\*\**p* < 0.001.

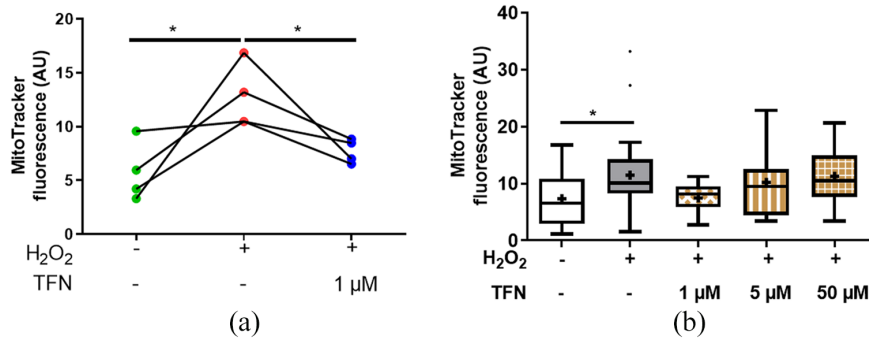


**Figure 5.** Teriflunomide (TFN) at 1 µM altered the oxidation potential of mitochondria, reducing oxidative MitoTracker Orange fluorescence intensity. Fluorescence intensity of MitoTracker Orange staining depicting significant reduction of oxidation potential of 1 µM TFN. (b) MitoTracker Orange fluorescence intensity at 1, 5 and 50 µM TFN treatment during oxidative stress in comparison with untreated and H<sub>2</sub>O<sub>2</sub>-treated roots. \*Statistical significance with *p* value < 0.05.

**Table 4.** Summary of mean fluorescence intensities of mitochondria.

	<i>n</i> =	MitoTracker fluorescence (AU)	Mann-Whitney test
Untreated	39	7.35 ± 4.76	*
H <sub>2</sub> O <sub>2</sub> -treated	44	11.49 ± 6.44	
H <sub>2</sub> O <sub>2</sub> + TFN (1 µM)	18	7.48 ± 2.75	*
H <sub>2</sub> O <sub>2</sub> + TFN (5 µM)	15	10.22 ± 6.45	>0.1
H <sub>2</sub> O <sub>2</sub> + TFN (50 µM)	21	11.27 ± 4.79	>0.1

AU, arbitrary units. Values are shown as mean ± SD. \**p* < 0.05.

immune system,<sup>25,35</sup> there is a general lack of treatment targeting inflammation-promoted neurodegeneration,<sup>36,37</sup> which is an integral component of disability progression.<sup>37,38</sup> As early mitochondrial alterations are reported in inflammatory neurodegenerative diseases,<sup>8,11–16</sup> the maintenance of mitochondrial integrity could be a key goal to achieve neuronal protection during neuroinflammation.<sup>39</sup> Here, we hypothesized that TFN, due to its ability to inhibit DHODH,<sup>40</sup> an enzyme functionally linked with complex III activity of the mitochondrial respiratory chain,<sup>41</sup> may influence mitochondrial stability in the context of oxidative stress. To test our hypothesis, we used our previously established model of murine explanted ventral roots, in which the morphology and the transport of mitochondria can be analyzed within peripheral axons.<sup>18,28</sup>

After excluding any relevant effect of DMSO (the dilution vehicle), in both untreated and H<sub>2</sub>O<sub>2</sub>-treated mitochondria (Supplemental Figures 1–2), we investigated the effect of TFN treatment in unmanipulated or oxidative stress-exposed spinal root explants.

Interestingly, in non-stressed roots, TFN seems to promote mitochondrial fusion, induce mitochondrial elongation (Figure 1d, e), and reduce mitochondrial velocity (Figure 2b). Mitochondrial fusion is important for the formation of mitochondrial networking that assists in reshuffling and redistributing the mitochondrial content.<sup>42,43</sup> Thus, the inhibition of DHODH and subsequent effects on complex III of the electron transport chain (ETC) and respiration<sup>41</sup> may promote mitochondrial fusion as an attempt to redistribute the electron transport complexes that are still capable of maintaining the proton gradient and synthesizing adenosine triphosphate (ATP).

In contrast, during oxidative stress, we observed a reduction in mitochondrial length and size, which is indicative of fragmentation/fission of mitochondria that might undergo mitophagy. Mitochondrial fission has also been proposed to increase the number of mitochondria and their cellular distribution in order to meet the increasing energy demands of the cell.<sup>44,45</sup> Although mitochondrial fission is extensively discussed in terms of mitophagy as well as apoptosis,<sup>43–46</sup> intensive mitochondrial fission may translate into mitochondrial failure and the strategy to optimize

mitochondrial functionality before undergoing apoptosis. It also serves to get rid of damaged, irreparable mitochondrial parts.<sup>45,47</sup> Importantly, in the presence of 1 μM and 50 μM TFN, reduction in mitochondrial length and area due to oxidative insult could be prevented (Figure 3g, h). Intensive fragmentation during oxidative stress could not be prevented with 5 μM TFN.

Further, consistent with previous findings, we observed a reduced mitochondrial motility during oxidative stress,<sup>14,18</sup> that is, reduced trajectories and transport velocity. The impairment of mitochondrial transport was preserved with TFN treatment. In axons, around 10–30% of mitochondria are motile, while more than 70% remain stationary.<sup>48</sup> This motile and stationary pool of mitochondria is dependent on the current energy demands of the cell.<sup>49,50</sup> In addition, disrupted motility could lead to impairment of mitochondrial fusion.<sup>46,49,51</sup> Thus, TFN may promote fusion by influencing the motility. On the other hand, it has been proposed that inhibition of DHODH by TFN may reduce the total amount of ROS in the cell.<sup>52</sup> Thus, TFN-mediated ROS reduction may also lead indirectly to an increased motility of stressed mitochondria.

Along this line, to assess the effects of TFN on ROS in our system, we monitored the fluorescence intensity of MitoTracker Orange CMTMRos (see Methods).<sup>34</sup> As expected, fluorescence intensity of CMTMRos significantly increased with H<sub>2</sub>O<sub>2</sub> treatment, while inhibition of DHODH with 1 μM TFN reduced the ROS level (Figure 5). As complex III of the ETC is considered one of the major contributors to ROS formation, its compromised activity in the presence of TFN might reduce ROS production in mitochondria in peripheral spinal root explants. 5 μM and 50 μM TFN could not effectively reduce ROS, which might be attributed to the inhibition at higher concentrations of additional signaling pathways including tyrosine kinases.<sup>53</sup>

On the other hand, the intermediate dose of 5 μM TFN showed no effects on H<sub>2</sub>O<sub>2</sub>-induced shape or motility changes. Why, in our experimental setup a dose effect is missing, remains uncertain. The high variability of our data, which is intrinsic to the nature of mitochondrial dynamics and reflects the heterogeneity of the mitochondrial population in both physiological and diseased conditions, could have contributed to mask a true dose effect. To minimize this problem, several experiments

with large amounts of mitochondria were analyzed (see Methods section). Moreover, depending on its concentration, TFN may function by a different mode of action. While low TFN concentrations are effective in inhibiting DHODH (1–1.5  $\mu\text{M}$ ), concentrations needed to achieve DHODH-independent effects such as inhibition of protein tyrosine kinase or cyclooxygenase-2 are much higher (50–200  $\mu\text{M}$ ).<sup>29</sup> However, little is known about the mode of action of intermediate concentrations. One could speculate that in our model, TFN at 5  $\mu\text{M}$  may achieve partially known or yet undefined DHODH-independent effects that rather counterbalance the beneficial effects observed at 1  $\mu\text{M}$ , while at 50  $\mu\text{M}$  DHODH-dependent and independent mechanisms may synergize against dysfunctions observed under oxidative stress. Future experiments using long-living explants are needed to evaluate to what extent TFN effects at different concentration are DHODH-dependent and thus reversible.

Our previous data on root explants demonstrated that mitochondrial alterations caused by oxidative stress precede axonal damage.<sup>18</sup> Now, we show that these alterations could be pharmacologically reversed *in vitro* by TFN. Targeting dysfunction of axonal mitochondria should become one of the key goals in drug development not only for MS but also for other classic neurodegenerative disorders such as Parkinson's or Alzheimer diseases.<sup>54</sup> In this line, we showed in the animal model of MS a protective effect of epigallocatechin-3-gallate (EGCG),<sup>55,56</sup> a polyphenol, that among others, inhibits the formation of ROS and protects neurons.<sup>57,58</sup> Also dimethyl fumarate, used to treat MS, prevents oxidative stress-related mitochondrial dysfunction, apoptosis and autophagy in murine oligodendrocytes *in vitro*.<sup>59</sup> Importantly, endogenous substances currently being investigated in MS may be exploited as therapeutics due their mitochondria-protective capacities, such as high dose biotin,<sup>60</sup> vitamin D<sup>61</sup> or octadecaneuropeptide, a neurotrophic peptide produced principally by astrocytes, which is able to counteract oxidative stress-induced alterations.<sup>62</sup>

In summary, our present findings suggest a protective effect of TFN on axonal mitochondria exposed to oxidative stress. Investigations expanding on these findings are needed to determine whether mitochondrial protection at the axonal level can be translated into protection of axons and neurons.

### Conflict of interest

The authors declare that there is no conflict of interest.

### Funding

The authors disclosed receipt of the following financial support for the research, authorship, and/or publication of this article: This work was funded by a research grant from Sanofi Genzyme to C.I-D. A.E.H, was supported by DFG TRR130, TP17. The authors also acknowledge support from the German Research Foundation (DFG) and the Open Access Publication Funds of Charité- Universitätsmedizin.

### ORCID iD

Carmen Infante-Duarte  <https://orcid.org/0000-0003-3005-351X>

### Supplemental material

Supplemental material for this article is available online.

### References

1. Chen AY, Chonghasawat AO and Leadholm KL. Multiple sclerosis: frequency, cost, and economic burden in the United States. *J Clin Neurosci* 2017; 45: 180–186.
2. Compston A and Coles A. Multiple sclerosis. *Lancet* 2008; 372: 1502–1517.
3. Dutta R and Trapp BD. Pathogenesis of axonal and neuronal damage in multiple sclerosis. *Neurology* 2007; 68 (Suppl. 3): S22–S31; discussion S43–S54.
4. Lublin FD, Reingold SC, Cohen JA, *et al.* Defining the clinical course of multiple sclerosis: the 2013 revisions. *Neurology* 2014; 83: 278–286.
5. Mäurer M and Rieckmann P. Relapsing–remitting multiple sclerosis: what is the potential for combination therapy? *BioDrugs* 2000; 13: 149–158.
6. Geurts JJG and Barkhof F. Grey matter pathology in multiple sclerosis. *Lancet Neurol* 2008; 7: 841–851.
7. Barsukova AG, Forte M and Bourdette D. Focal increases of axoplasmic Ca<sup>2+</sup>, aggregation of sodium–calcium exchanger, N-type Ca<sup>2+</sup> channel, and actin define the sites of spheroids in axons undergoing oxidative stress. *J Neurosci* 2012; 32: 12028–12037.

8. Coleman M. Axon degeneration mechanisms: commonality amid diversity. *Nat Rev Neurosci* 2005; 6: 889–898.
9. Mossakowski AA, Pohlan J, Bremer D, *et al.* Tracking CNS and systemic sources of oxidative stress during the course of chronic neuroinflammation. *Acta Neuropathol* 2015; 130: 799–814.
10. Fischer MT, Wimmer I, Höftberger R, *et al.* Disease-specific molecular events in cortical multiple sclerosis lesions. *Brain* 2013; 136: 1799–1815.
11. Nikić I, Merkler D, Sorbara C, *et al.* A reversible form of axon damage in experimental autoimmune encephalomyelitis and multiple sclerosis. *Nat Med* 2011; 17: 495–499.
12. Mahad D, Ziabreva I, Lassmann H, *et al.* Mitochondrial defects in acute multiple sclerosis lesions. *Brain* 2008; 131: 1722–1735.
13. Court FA and Coleman MP. Mitochondria as a central sensor for axonal degenerative stimuli. *Trends Neurosci* 2012; 35: 364–372.
14. Fang C, Bourdette D and Banker G. Oxidative stress inhibits axonal transport: implications for neurodegenerative diseases. *Mol Neurodegener* 2012; 7: 29.
15. Medana IM and Esiri MM. Axonal damage: a key predictor of outcome in human CNS diseases. *Brain* 2003; 126: 515–530.
16. Saxton WM and Hollenbeck PJ. The axonal transport of mitochondria. *J Cell Sci* 2012; 125: 2095–2104.
17. Campbell GR, Ziabreva I, Reeve AK, *et al.* Mitochondrial DNA deletions and neurodegeneration in multiple sclerosis. *Ann Neurol* 2011; 69: 481–492.
18. Bros H, Millward JM, Paul F, *et al.* Oxidative damage to mitochondria at the nodes of Ranvier precedes axon degeneration in ex vivo transected axons. *Exp Neurol* 2014; 261: 127–135.
19. Armstrong JA, Cash NJ, Ouyang Y, *et al.* Oxidative stress alters mitochondrial bioenergetics and modifies pancreatic cell death independently of cyclophilin D, resulting in an apoptosis-to-necrosis shift. *J Biol Chem* 2018; 293: 8032–8047.
20. Miller AE, Wolinsky JS, Kappos L, *et al.* Oral teriflunomide for patients with a first clinical episode suggestive of multiple sclerosis (TOPIC): a randomised, double-blind, placebo-controlled, phase 3 trial. *Lancet Neurol* 2014; 13: 977–986.
21. O'Connor P, Wolinsky JS, Confavreux C, *et al.* Randomized trial of oral teriflunomide for relapsing multiple sclerosis. *N Engl J Med* 2011; 365: 1293–1303.
22. Bar-Or A. Teriflunomide (Aubagio®) for the treatment of multiple sclerosis. *Exp Neurol* 2014; 262: 57–65.
23. Li L, Liu J, Delohery T, *et al.* The effects of teriflunomide on lymphocyte subpopulations in human peripheral blood mononuclear cells in vitro. *J Neuroimmunol* 2013; 265: 82–90.
24. Warnke C, zu Hörste GM, Hartung HP, *et al.* Review of teriflunomide and its potential in the treatment of multiple sclerosis. *Neuropsychiatr Dis Treat* 2009; 5: 333–340.
25. Warnke C, Stüve O and Kieseier BC. Teriflunomide for the treatment of multiple sclerosis. *Clin Neurol Neurosurg* 2013; 115 (Suppl. 1): S90–S94.
26. Zivadinov R, Bergsland N, Carl E, *et al.* Effect of teriflunomide and dimethyl fumarate on cortical atrophy and leptomeningeal inflammation in multiple sclerosis: a retrospective, observational, case-control pilot study. *J Clin Med* 2019; 8: 344.
27. Rzagalinski I, Hainz N, Meier C, *et al.* Spatial and molecular changes of mouse brain metabolism in response to immunomodulatory treatment with teriflunomide as visualized by MALDI-MSI. *Anal Bioanal Chem* 2019; 411: 353–365.
28. Bros H, Niesner R and Infante-Duarte C. An ex vivo model for studying mitochondrial trafficking in neurons. *Methods Mol Biol* 2015; 1264: 465–472.
29. Oh J and O'Connor PW. An update of teriflunomide for treatment of multiple sclerosis. *Ther Clin Risk Manag* 2013; 9: 177–190.
30. Kaplan J, Cavalier S and Turpault S. Biodistribution of teriflunomide in naive rats vs rats with experimental autoimmune encephalomyelitis. *ECTRIMS Online Library*, 2015.
31. Palmer AM. Efficacy and safety of teriflunomide in treatment of multiple sclerosis. *J Symptoms Signs* 2013; 2: 444–457.
32. Zierle J, Bissinger R and Lang F. Inhibition by teriflunomide of erythrocyte cell membrane scrambling following energy depletion, oxidative stress and ionomycin. *Cell Physiol Biochem* 2016; 39: 1877–1890.

33. Bros H, Hauser A, Paul F, *et al.* Assessing mitochondrial movement within neurons: manual versus automated tracking methods. *Traffic* 2015; 16: 906–917.
34. Kweon SM, Kim HJ, Lee ZW, *et al.* Real-time measurement of intracellular reactive oxygen species using mito tracker orange (CMH2TMRos). *Biosci Rep* 2001; 21: 341–352.
35. Breedveld FC and Dayer JM. Leflunomide: mode of action in the treatment of rheumatoid arthritis. *Ann Rheum Dis* 2000; 59: 841–849.
36. Claussen MC and Korn T. Immune mechanisms of new therapeutic strategies in MS: teriflunomide. *Clin Immunol* 2012; 142: 49–56.
37. Rudick RA and Trapp BD. Gray-matter injury in multiple sclerosis. *N Engl J Med* 2009; 361: 1505–1506.
38. Aktas O, Smorodchenko A, Brocke S, *et al.* Neuronal damage in autoimmune neuroinflammation mediated by the death ligand TRAIL. *Neuron* 2005; 46: 421–432.
39. Moreira PI, Zhu X, Wang X, *et al.* Mitochondria: a therapeutic target in neurodegeneration. *Biochim Biophys Acta* 2010; 1802: 212–220.
40. Fang J, Uchiumi T, Yagi M, *et al.* Dihydroorotate dehydrogenase is physically associated with the respiratory complex and its loss leads to mitochondrial dysfunction. *Biosci Rep* 2013; 33: e00021.
41. Khutorenko AA, Dalina AA, Chernyak BV, *et al.* The role of dihydroorotate dehydrogenase in apoptosis induction in response to inhibition of the mitochondrial respiratory chain complex III. *Acta Naturae* 2014; 6: 69–75.
42. Rafelski SM. Mitochondrial network morphology: building an integrative, geometrical view. *BMC Biol* 2013; 11: 71.
43. Chan DC. Fusion and fission: interlinked processes critical for mitochondrial health. *Annu Rev Genet* 2012; 46: 265–287.
44. Kaasik A, Safulina D, Choubey V, *et al.* Mitochondrial swelling impairs the transport of organelles in cerebellar granule neurons. *J Biol Chem* 2007; 282: 32821–32826.
45. Safulina D and Kaasik A. Energetic and dynamic: how mitochondria meet neuronal energy demands. *PLoS Biol* 2013; 11: e1001755.
46. Detmer SA and Chan DC. Functions and dysfunctions of mitochondrial dynamics. *Nat Rev Mol Cell Biol* 2007; 8: 870–879.
47. Chan DC. Mitochondria: dynamic organelles in disease, aging, and development. *Cell* 2006; 125: 1241–1252.
48. Misgeld T, Kerschensteiner M, Bareyre FM, *et al.* Imaging axonal transport of mitochondria in vivo. *Nat Methods* 2007; 4: 559–561.
49. Schwarz TL. Mitochondrial trafficking in neurons. *Cold Spring Harb Perspect Biol* 2013; 5: a011304.
50. Ohno N, Kidd GJ, Mahad D, *et al.* Myelination and axonal electrical activity modulate the distribution and motility of mitochondria at CNS nodes of Ranvier. *J Neurosci* 2011; 31: 7249–7258.
51. Cagalinec M, Safulina D, Liiv M, *et al.* Principles of the mitochondrial fusion and fission cycle in neurons. *J Cell Sci* 2013; 126: 2187–2197.
52. Fairus AKM, Choudhary B, Hosahalli S, *et al.* Dihydroorotate dehydrogenase (DHODH) inhibitors affect ATP depletion, endogenous ROS and mediate S-phase arrest in breast cancer cells. *Biochimie* 2017; 135: 154–163.
53. Herrmann ML, Schleyerbach R and Kirschbaum BJ. Leflunomide: an immunomodulatory drug for the treatment of rheumatoid arthritis and other autoimmune diseases. *Immunopharmacology* 2000; 47: 273–289.
54. Area-Gomez E, Guardia-Laguarta C, Schon EA, *et al.* Mitochondria, OxPhos, and neurodegeneration: cells are not just running out of gas. *J Clin Invest* 2019; 129: 34–45.
55. Janssen A, Fiebiger S, Bros H, *et al.* Treatment of chronic experimental autoimmune encephalomyelitis with epigallocatechin-3-gallate and glatiramer acetate alters expression of heme-oxygenase-1. *PLoS One* 2015; 10: e0130251.
56. Herges K, Millward JM, Hentschel N, *et al.* Neuroprotective effect of combination therapy of glatiramer acetate and epigallocatechin-3-gallate in neuroinflammation. *PLoS One* 2011; 6: e25456.
57. Aktas O, Prozorovski T, Smorodchenko A, *et al.* Green tea epigallocatechin-3-gallate mediates T cellular NF- $\kappa$ B inhibition and exerts neuroprotection in autoimmune encephalomyelitis. *J Immunol* 2004; 173: 5794–5800.
58. Schroeder EK, Kelsey NA, Doyle J, *et al.* Green tea epigallocatechin 3-gallate accumulates in mitochondria and displays a selective antiapoptotic effect against inducers of mitochondrial oxidative stress in neurons. *Antioxid Redox Signal* 2009; 11: 469–480.
59. Sghaier R, Nury T, Leoni V, *et al.* Dimethyl fumarate and monomethyl fumarate


attenuate oxidative stress and mitochondrial alterations leading to oxiaoptophagy in 158N murine oligodendrocytes treated with 7 $\beta$ -hydroxycholesterol. *J Steroid Biochem Mol Biol* 2019; 194: 105432.

60. Sedel F, Bernard D, Mock DM, *et al.* Targeting demyelination and virtual hypoxia with high-dose biotin as a treatment for progressive multiple sclerosis. *Neuropharmacology* 2016; 110: 644–653.

61. Rodney C, Rodney S and Millis RM. Vitamin D and demyelinating diseases: neuromyelitis optica (NMO) and multiple sclerosis (MS). *Autoimmune Dis* 2020; 2020: 8718736.

62. Namsi A, Nury T, Khan AS, *et al.* Octadecaneuropeptide (ODN) induces N2a cells differentiation through a PKA/PLC/PKC/MEK/ERK-dependent pathway: incidence on peroxisome, mitochondria, and lipid profiles. *Molecules* 2019; 24: 3310.

Visit SAGE journals online  
[journals.sagepub.com/  
home/taj](https://journals.sagepub.com/home/taj)

 SAGE journals